A R C H I V E S O F M E T A L L U R G Y A N D M A T E R I A L S
Volume 57 2012 Issue 2
DOI: 10.2478/v10172-012-0042-3

A. HALLOUMI*, CH. DESRAYAUD*, B. BACROIX**, E. RAUCH***, F. MONTHEILLET*

A SIMPLE ANALYTICAL MODEL OF ASYMMETRIC ROLLING

PROSTY MODEL ANALITYCZNY ASYMETRYCZNAGO WALCOWANIA

An original analytical method is proposed for modeling asymmetric rolling (ASR) of metal sheet. It is based on a uniform strain field depending on a single optimization parameter, viz. the entry velocity of the sheet. The shear and normal strains associated with an ASR pass are derived analytically. Moreover, it is shown that the entry velocity almost coincides with the outer linear velocity of the slower roll, as far as ASR is sufficiently asymmetric. In that case, closed form formulae are available for the main rolling parameters such as the overall power dissipated and the two rolling torques. These results can be straighforwardly used for practical applications.

Keywords: Asymmetric rolling, upper bound method, uniform strain field method

Zaproponowano oryginalną metodę analityczną do modelowania asymetrycznego walcowania blachy. Model jest oparty na jednolitym obszarze odkształcenia zależnym od jednego parametru optymalizacji tj. prędkości wejścia arkusza. Naprężenia ścinanające i normalne związane z przebiegiem asymetrycznego walcowania wyprowadzone są analitycznie. Co więcej, pokazano, że prędkość wejścia niemal zbiega się z zewnętrzną prędkością liniową wolniejszego walca, o ile asymetryczne walcowanie jest wystarczająco asymetryczne. W takim przypadku zamknięte równania są dostępne dla głównych parametrów walcowania takich jak całkowita moc rozpraszania i dwa momenty obrotowe walcowania. Wyniki te mogą być bezpośrednio wykorzystywane do zastosowań praktycznych.

C_1, C_2	Rolling torque of the upper and lower rolls, respectively
$2h_e$,$2h_f$	Initial and final sheet thicknesses
h_1, h_2	Upper and lower material thicknesses with respect to the horizontal axis, respectively
L	Roll gap length
$\overline{m}_1$, $\overline{m}_2$	Tresca friction coefficients of the upper and lower rolls, respectively
R_1, R_2	Radius of the upper and lower rolls, respectively
$\dot{u}_e$	Material velocity at entrance of the roll gap
$\dot{u}_f$	Material (final) velocity at exit of the roll gap
$\dot{u}_1$, $\dot{u}_2$	Material velocity at the top and bottom exit points, respectively
V_r	Roll rotation velocity ratio
W_P, W_F, W_D	Plastic, friction, and discontinuity power, respectively
λ	Reduction ratio
$\dot{\Omega}_1$, $\dot{\Omega}_2$	Angular velocities of the upper and lower rolls, respectively

* ECOLE DES MINES DE SAINT-ETIENNE (CENTRE SMS), CNRS UMR 5146, FRANCE
** LPMTM, UNIVERSITÉ PARIS 13, CNRS, FRANCE
*** SIMAP/GPM2, CNRS-UJF, SAINT MARTIN D'HÈRES, FRANCE

1. Introduction

Asymmetric rolling (ASR) is a new promising process for the manufacturing of metal sheets and strips. It can be achieved by using rolls of unequal diameters, by prescribing different speeds of rotation to the rolls, by imposing different friction coefficients between the two rolls and the sheet, or else by a combination of these various factors. In cold working, the major effect of asymmetry is to impose an additional shear strain to the material, which in turn modifies the final microstructure and texture. In particular, it may lead to considerable grain refinement after subsequent heat treatment [1]. In the field of hot working, this process has also been used to counterbalance local shears close to the skin of the sheet and avoid sheet bending [2].

Early analytical studies of ASR have been performed by Sachs and Klinger [3], where the slab method was used to develop a homogenous deformation model. This model has been extended by Holbrook and Zorowski [4], including dissymmetry of the roll pressure distribution. Their model can predict the output strip curvature. Boxton and Browning [5] rolled strips of plasticine, and Chekmarev and Nefedov [6] conducted tests with lead, steel and aluminium. Their results showed that under some conditions, a 40% reduction of the rolling force is possible. Ghobrial [7] used the technique of photo-elasticimetry and an experimental method to measure contact stresses, during plane strain ASR. He concluded that the asymmetry due to difference in roll radii had no significant effect on the size of the cross shear zone. Hwang et al. [8], have proposed an analytical model for asymmetric cold rolling of sheet using the stream function method and the upper bound theorem, to investigate the plastic behaviour of the sheet at the roll-gap. In parallel, experiments on ASR were also conducted on aluminium, copper, and steel. Moreover, analytical modeling and experimental investigations of ASR have been performed by Hwang and Tzou [9, 10]. They developed a model based on the slab method for ASR, assuming constant shear friction between the rolls and the sheet. In another paper, Tzou [11] studied the relationship between the Tresca and Coulomb friction coefficients. Moreover, the effects of rolling conditions on this relationship were investigated.

Salimi and co-workers analyzed ASR with different methods. First of all, they used the slab method [12]. The authors also proposed two possible physical methods to ensure horizontal entrance of the plate [13]. In another paper, simulation of ASR was carried out using the finite element method for predicting the sheet curvature due to the inequality in roll speeds and interface frictions, in the case of isotropic work-hardening material [14]. Furthermore, slab analysis and genetic algorithms were also used for modeling ASR [15].

Finally, several researchers have selected the finite element method for modeling ASR. Richelsen [15] concluded that curvature increases with the reduction ratio for ratios less than about 30%, while it decreases for larger ratios. Lu et al. [17] studied the effects of the roll speeds and roll diameters on curvature, using an elastic-plastic finite element analysis. Three-dimensional numerical analysis was also performed by Akbari Mousavi and co-workers [18]. The authors concluded that increasing the rotation velocity ratio, increases the length of the shear zone.

In this paper, an analytical method based on uniform strain field depending on one unique parameter is proposed to determine the overall quantities relevant to a single pass of ASR, *viz*. the normal and shear strains, as well as the required powers and torques. It mainly leads to closed form equations that can be straightforwardly used for ASR practice.

2. Mathematical model

The development of a simple mathematical model for asymmetric hot rolling requires the most general following assumptions:

(i) The rolls are considered to be rigid bodies, and the rolled material rigid-perfectly plastic, possibly temperature dependent.
(ii) Plane strain deformation is applied.
(iii) The flow directions of the strip at the entrance and exit of the roll gap are both horizontal. Bending effects of the rolled sheet are therefore neglected.
(iv) The total roll contact arc is much smaller than the circumference of the roll.

The approach proposed in this paper is also referred to as the method of uniform energy. It first consists to estimate the average values of the mechanical parameters as a function of the entrance velocity $\dot{u}_e$ of the sheet, then to derive the value of $\dot{u}_e$ which minimizes the total power dissipated by the system. It has already been used for conventional rolling [19].

2.1. Geometry and kinematics

Let $\dot{\Omega}_1$ and $\dot{\Omega}_2$ denote the rotation rates of the upper and lower cylinders, of respective radii R_1 and R_2 (Fig. 1; see also Fig. A1 in Appendix A). The exit (final) velocity $\dot{u}_f$ is assumed to vary linearly from $\dot{u}_1$ at the top to $\dot{u}_2$ at the bottom of the sheet, with $\dot{u}_1 = \dot{u}_e + \eta\dot{\Omega}_1 R_1$ and $\dot{u}_2 = \dot{u}_e + \eta\dot{\Omega}_2 R_2$, respectively, where $\dot{\Omega}_1 R_1$ and $\dot{\Omega}_2 R_2$ are the outer tangential velocities of the cylinders. Because of volume conservation, the average velocity $(\dot{u}_1 + \dot{u}_2)/2$

must equal $\lambda \dot{u}_e$, where $\lambda = h_e/h_f$ is the reduction ratio (h_e and h_f are the entrance and final half-thicknesses, respectively). Combining these equations determines the value of η, hence leading to:

$$\dot{u}_1 = \frac{(2\lambda - 1)\,\dot{\Omega}_1 R_1 + \dot{\Omega}_2 R_2}{\dot{\Omega}_1 R_1 + \dot{\Omega}_2 R_2}\dot{u}_e$$
$$\dot{u}_2 = \frac{\dot{\Omega}_1 R_1 + (2\lambda - 1)\,\dot{\Omega}_2 R_2}{\dot{\Omega}_1 R_1 + \dot{\Omega}_2 R_2}\dot{u}_e \quad (1)$$

The average length L of a material trajectory between the cylinders can be derived from geometrical considerations (Appendix A). When the cylinder diameters are similar, a rough estimation gives $L^2 = \left(h_e - h_f\right)\left[2R - \left(h_e - h_f\right)\right]$, where R stands for the

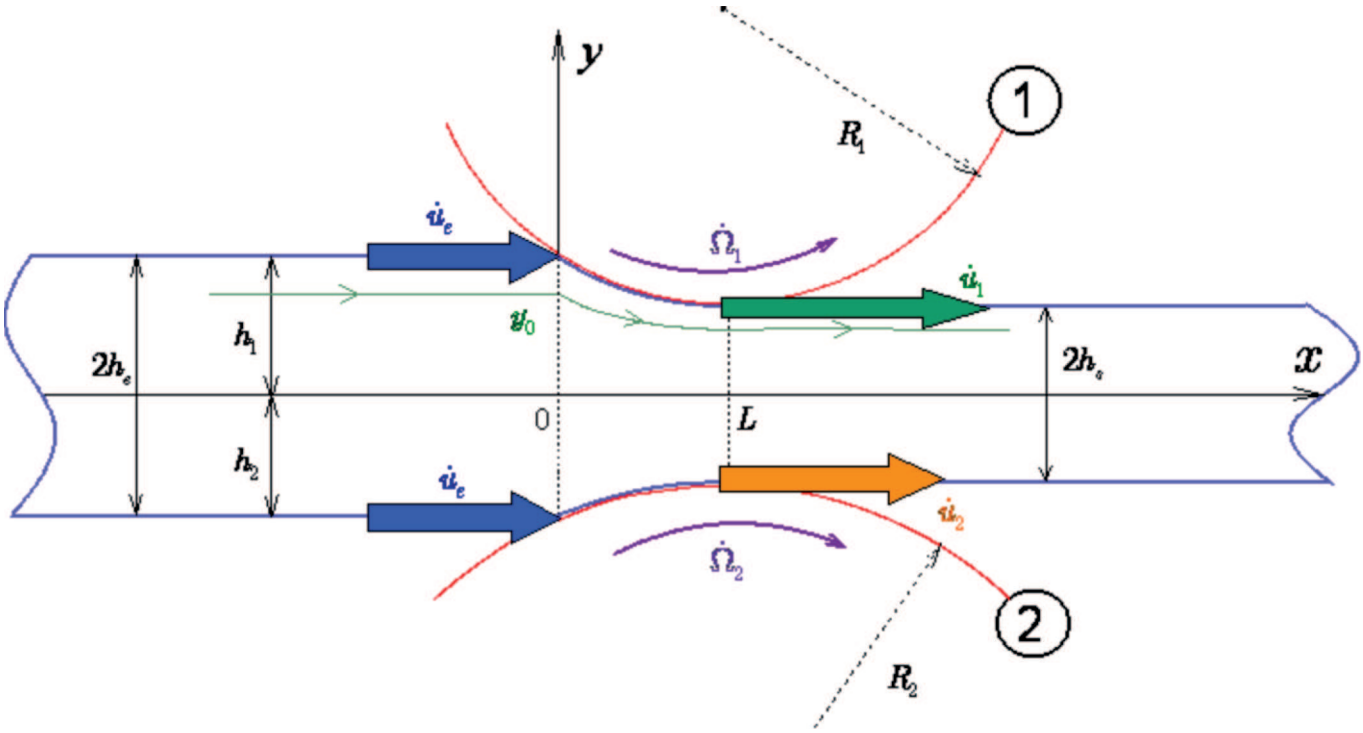

Fig. 1. Schematic representation of the asymmetric rolling geometry

average cylinder radius. For the average velocity is $(\lambda + 1)\,\dot{u}_e/2$, the associated time interval is:

$$\Delta t = \frac{2}{\lambda + 1}\frac{L}{\dot{u}_e} \quad (2)$$

2.2. Strains and strain rates

To a first approximation, $\varepsilon_{xx} = -\varepsilon_{yy} = \ln\frac{h_e}{h_f} = \ln\lambda$, whence:

$$\dot{\varepsilon}_{xx} = -\dot{\varepsilon}_{yy} = \frac{\varepsilon_{xx}}{\Delta t} = \frac{\lambda + 1}{2}\ln\lambda\frac{\dot{u}_e}{L} \quad (3)$$

(Note that, although for given $\dot{u}_e$ this formula does not differ from classical rolling, asymmetry is accounted for by the specific value of $\dot{u}_e$, as will be seen below). The average shear strain rate $\dot{\gamma} = 2\dot{\varepsilon}_{xy}$ can be estimated in turn by:

$$\dot{\gamma} = \frac{[(\dot{u}_e + \dot{u}_1)/2] - [(\dot{u}_e + \dot{u}_2)/2]}{h_e + h_f} = \frac{\lambda(\lambda - 1)}{\lambda + 1}\Delta\frac{\dot{u}_e}{h_e} \quad (4)$$

in which $\Delta = \frac{\dot{\Omega}_1 R_1 - \dot{\Omega}_2 R_2}{\dot{\Omega}_1 R_1 + \dot{\Omega}_2 R_2}$. Accordingly, the total shear applied to the material is:

$$\gamma = \dot{\gamma}\Delta t = \frac{2\lambda(\lambda - 1)}{(\lambda + 1)^2}\Delta\frac{L}{h_e} \quad (5)$$

For estimating the degree of asymmetry, it is usual to introduce a parameter $a = \dot{\gamma}/\dot{\varepsilon}_{xx}$ ($=\gamma/\varepsilon_{xx}$ in the present model), which takes the value:

$$a = \frac{2\lambda(\lambda - 1)}{(\lambda + 1)^2\ln\lambda}\Delta\frac{L}{h_e} \quad (6)$$

From Eqs (3) and (4) it is easy to derive the average von Mises equivalent strain rate in asymmetric rolling:

$$\dot{\bar{\varepsilon}} = \frac{2}{\sqrt{3}}\sqrt{\dot{\varepsilon}_{xx}^2 + \dot{\gamma}^2/4} = \frac{2}{\sqrt{3}}\dot{\varepsilon}_{xx}\sqrt{1 + a^2/4} \quad (7)$$

and the associated von Mises equivalent strain:

$$\bar{\varepsilon} = \frac{2}{\sqrt{3}} \ln \lambda \sqrt{1 + a^2/4} \tag{8}$$

Another relevant and easily measurable parameter is the *apparent shear strain* γ_{app}: if a straight line initially parallel to the y-axis makes an angle θ with the latter after rolling, γ_{app} - tan θ. In view of the present assumptions:

$$\gamma_{app} = \frac{(\dot{u}_1 - \dot{u}_2)\,\Delta t}{4h_f} = \frac{\lambda(\lambda - 1)}{\lambda + 1}\Delta\frac{L}{h_e} \tag{9}$$

Using Eqs (6) and (9), the equivalent strain can be reformulated in the form:

$$\bar{\varepsilon} = \frac{2}{\sqrt{3}} \ln \lambda \sqrt{1 + \left[\frac{\gamma_{app}}{(\lambda + 1)\ln\lambda}\right]^2} \tag{10}$$

The above equation can be compared with the expression proposed by Saito *et al.* [20] and used by Cui and Ohori [21] (Appendix B):

$$\gamma_{app} = a\frac{r(2 - r)}{2(1 - r)^2} \tag{11}$$

in which $r=1-h_f/h_e=1-1/\lambda$, and a is still defined by $a=\dot{\gamma}/\dot{\varepsilon}_{xx}$. Hence for these authors:

$$\bar{\varepsilon} = \frac{2}{\sqrt{3}} \ln \frac{1}{1 - r} \sqrt{1 + \left[\frac{(1 - r)^2}{r(2 - r)}\gamma_{app}\right]^2} \tag{12}$$

which can be written in the equivalent form:

$$\bar{\varepsilon} = \frac{2}{\sqrt{3}} \ln \lambda \sqrt{1 + \left[\frac{\gamma_{app}}{\lambda^2 - 1}\right]^2} \tag{13}$$

It is easy to check that Eqs (10) and (13) are equivalent for low reduction ratios.

Finally, it is interesting to note that the above strains $\varepsilon_{xx}, \varepsilon_{xy} = \gamma/2$, and $\bar{\varepsilon}$ do not depend on the entrance velocity $\dot{u}_e$.

2.3. Power dissipated

The plastic power is given by $\dot{W}_p = \sigma_0 \dot{\bar{\varepsilon}} V$, where σ_0 is the material flow stress and V the volume of the plastic zone, i.e. $V \approx \left(h_e + h_f\right) L = h_e\,(1 + 1/\lambda)\,L$.

The power dissipated by friction $\dot{W}_F$ at the contact surfaces between the material sheet and the cylinders is more difficult to estimate. For that purpose, the Tresca friction model will be used, in which:

$$\dot{W}_F = \frac{\bar{m}\sigma_0}{\sqrt{3}} \int_0^L |\Delta\dot{u}|\, dx \tag{14}$$

in which $\bar{m}$ is the Tresca friction coefficient $(0 \leqslant \bar{m} \leqslant 1)$, $\Delta\dot{u} = \dot{\Omega}R - \dot{u}$ is the difference between the cylinder outer tangential velocity and the local velocity of the material element in contact. In consistency with the above assumptions, the latter is assumed to increase linearly with x:

$$\dot{u} = \dot{u}_e + (\dot{u}_f - \dot{u}_e)\,(x/L) \tag{15}$$

in which $\dot{u}_f = \dot{u}_1$ or $\dot{u}_2$ for the upper and lower cylinders, respectively. The point where $\Delta\dot{u} = 0$ is known as the *neutral point* of coordinate x_N. For a cylinder of radius R and rotation rate $\dot{\Omega}$, three cases must then be considered: (a) $\dot{u}_e < \dot{u}_f < \dot{\Omega}R$: the sheet is driven by the roll at any point and there is therefore no neutral point ($x_N > L$). Then $|\Delta\dot{u}| = \dot{\Omega}R - \dot{u}_e - (\dot{u}_f - \dot{u}_e)\,(x/L)$ and:

$$\dot{W}_F = \frac{\bar{m}\sigma_0}{\sqrt{3}}\left(\dot{\Omega}R - \frac{\dot{u}_e + \dot{u}_f}{2}\right)L \tag{16}$$

(b) $\dot{u}_e < \dot{\Omega}R < \dot{u}_f$: there is a neutral point given by:

$$x_N = \frac{\dot{\Omega}R - \dot{u}_e}{\dot{u}_f - \dot{u}_e}L \tag{17}$$

For $0 \leqslant x \leqslant x_N$, the sheet movement is driven by the roll, whereas for $x_N \leqslant x \leqslant L$, it is restrained by the latter; then $|\Delta\dot{u}| = \dot{\Omega}R - \dot{u}_e - (\dot{u}_f - \dot{u}_e)\,(x/L)$ and $|\Delta\dot{u}| = \dot{u}_e + (\dot{u}_f - \dot{u}_e)\,(x/L) - \dot{\Omega}R$, respectively and:

$$\dot{W}_F = \frac{\bar{m}\sigma_0}{\sqrt{3}}\frac{\dot{u}_e^2 + \dot{u}_f^2 - 2\dot{\Omega}R\left(\dot{u}_e + \dot{u}_f\right) + 2\dot{\Omega}^2R^2}{2\left(\dot{u}_f - \dot{u}_e\right)}L \tag{18}$$

(c) $\dot{\Omega}R < \dot{u}_e < \dot{u}_f$: the roll opposes the sheet movement at any point. There is therefore again no neutral point ($x_N \leqslant 0$). Then $|\Delta\dot{u}| = \dot{u}_e + (\dot{u}_f - \dot{u}_e)\,(x/L) - \dot{\Omega}R$ and:

$$\dot{W}_F = \frac{\bar{m}\sigma_0}{\sqrt{3}}\left(\frac{\dot{u}_e + \dot{u}_f}{2} - \dot{\Omega}R\right)L \tag{19}$$

The last power term is associated with the velocity discontinuity $\Delta\dot{u}_e$ occurring at the entrance of the sheet. The latter takes a maximum value at the sheet surface, which can be roughly estimated as $\Delta\dot{u}_e\,\max = \dot{u}_e \sin\theta \approx \dot{u}_e\theta \approx \dot{u}_e L/R$ (R is the average cylinder radius). Assuming that $\Delta\dot{u}_e$ varies linearly along the sheet depth, this gives:

$$\dot{W}_D = \frac{2\sigma_0}{\sqrt{3}}\int_0^{h_e} |\Delta\dot{u}_e| dy = \frac{\sigma_0}{\sqrt{3}}\frac{\dot{u}_e h_e L}{R} \tag{20}$$

Finally, the total power dissipated can be written in the form:

$$\dot{W} = \dot{W}_p + \dot{W}_{F1} + \dot{W}_{F2} + \dot{W}_D \tag{21}$$

and the entrance velocity $\dot{u}_e$ is determined by minimization of $\dot{W}$.

2.4. Rolling torques

Another expression of the total power is:

$$\dot{W} = C_1\dot{\Omega}_1 + C_2\dot{\Omega}_2 \qquad (22)$$

in which C_1 and C_2 are the torques prescribed by the upper and lower cylinder, respectively. Therefore:

$$C_1 = \frac{\partial \dot{W}}{\partial \dot{\Omega}_1} \quad \text{and} \quad C_2 = \frac{\partial \dot{W}}{\partial \dot{\Omega}_2} \qquad (23)$$

3. Results

In the following, the two rolls are assumed to have same radius $R_1 = R_2 = 100$ mm, the speed of revolution of the upper roll, $\dot{\Omega}_1 = 15$ tr.mn^{-1}, is constant, h_e=10 mm, and $\bar{m}_1 = \bar{m}_2$=1 (sticking contact between the cylinders and the sheet). The various quantities are plotted in function of the ratio $V_r = \dot{\Omega}_2/\dot{\Omega}_1$, which varies between 0 (the lower cylinder is stuck) up to 1 (symmetric rolling). Two rolling reductions are used, *i.e.* r = 0.1 (λ = 1.11), and r = 0.2 (λ = 1.25). This leads to L = 14.11 and 19.85 mm, respectively.

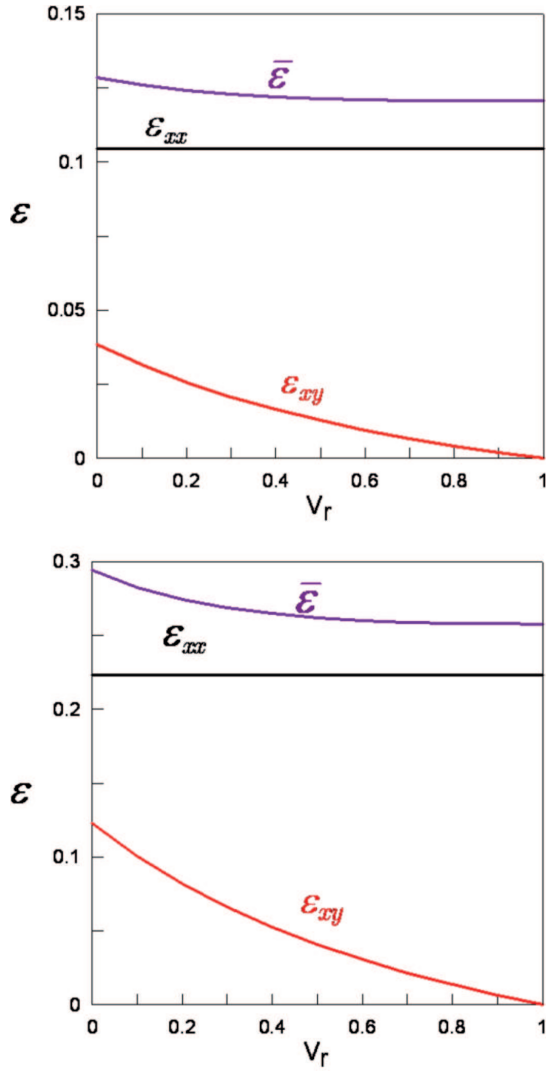

Fig. 2. Influence of the roll rotation velocity ratio on the normal, shear, and von Mises equivalent strains for two reductions ratios: (a) λ = 1.11 (r = 0.1), and (b) λ = 1.25 (r = 0.2)

For the above two test cases, Figures 2a and b show the dependence of the strains ε_{xx}, ε_{xy}, and $\bar{\varepsilon}$ on V_r. As expected, the shear strain ε_{xy} increases when the process departs from symmetric rolling, but it remains much lower than the main component ε_{xx}. The various components of power dissipated, *i.e.* $\dot{W}_P, \dot{W}_{F1}, \dot{W}_{F2}$, and $\dot{W}_D$, as well as the total power $\dot{W}$, are displayed in Fig. 3 for r = 0.2 and the associated velocities $\dot{u}_e, \dot{u}_1$, and $\dot{u}_2$ are shown in Fig. 4a and b for r = 0.2 and 0.1, respectively. For each value of V_r, $\dot{u}_e$ was numerically determined by minimization of $\dot{W}$. For weakly asymmetric rolling ($0.8 < V_r < 1$) , $\dot{W}$ is not much affected by Vr. By contrast, it appears that for strongly asymmetric rolling (V_r <0.8), W grows continuously due to the dramatic increase of $\dot{W}_{f1}$, while the speed of rolling (and the plastic power) tends to zero.

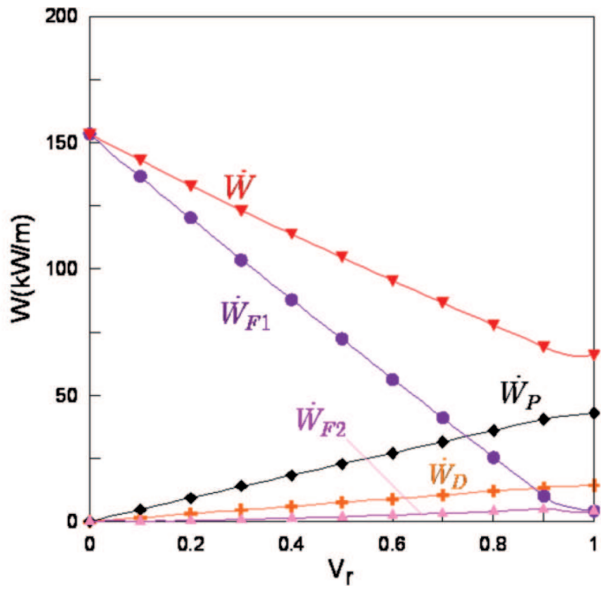

Fig. 3. Influence of the roll rotation velocity ratio on the various components of power dissipated, *viz.* the plastic $\dot{W}_P$, the friction $\dot{W}_1$ and $\dot{W}_2$, and the discontinuity power $\dot{W}_D$

Furthermore, Fig. 4a shows that the optimum entry velocity $\dot{u}_e$ is close to $\dot{\Omega}_2 R_2$ within the field of strongly asymmetric rolling, which becomes even more obvious when a lower reduction ratio is considered (Fig. 4b). This means that the lower cylinder opposes the sheet velocity over its total length of contact, whereas the upper cylinder exerts a positive driving force at any point (Figs 4a and b).

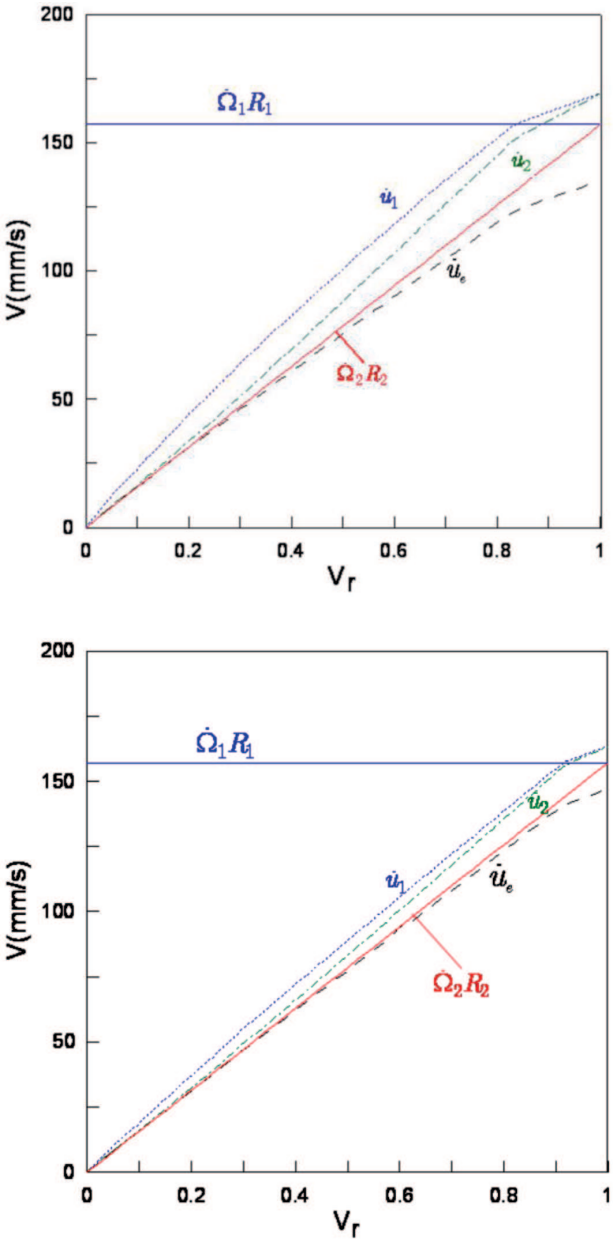

Fig. 4. Influence of the roll rotation velocity ratio on the entry velocity $\dot{u}_e$, and the upper and lower exit velocities $\dot{u}_1$, and $\dot{u}_2$, respectively. The outer linear velocity of the lower (and slower) cylinder $\dot{\Omega}_2 R_2$ is also shown

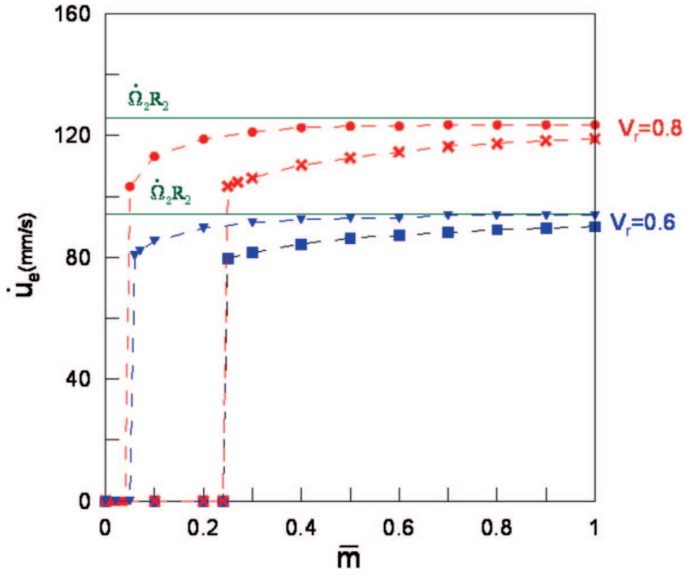

Fig. 5. Influence of the friction coefficient $\bar{m}$ on the entry velocity for two degrees of asymmetry V_r = 0.6 and 0.8

Figure 5 shows that $\dot{u}_e \approx \dot{\Omega}_2 R_2$ as long as the friction coefficient $\bar{m}$ is sufficiently large: $\bar{m} > \bar{m}_c$. The critical value $\bar{m}_c$ decreases with the initial sheet thickness. When $\bar{m} < \bar{m}_c$, the optimum $\dot{u}_e$ value falls to zero, which means that the friction shear stress is too low to drive the sheet into the roll gap.

Assuming $\dot{u}_e = \dot{\Omega}_2 R_2$, $R_1 = R_2 = R$, and $\bar{m}_1 = \bar{m}_2 = \bar{m}$, closed form expressions can be derived for the power dissipated and thus for the rolling torques under conditions of strongly asymmetric rolling:

$$\dot{W}_p = \frac{\sigma_0}{\sqrt{3}} \frac{\lambda + 1}{\lambda} h_e L \Theta^{1/2} \dot{\Omega}_2 \tag{24a}$$

$$\dot{W}_{F1} = \frac{\bar{m}\sigma_0 R}{\sqrt{3}} \left(\dot{\Omega}_1 - \dot{\Omega}_2 \frac{\lambda \dot{\Omega}_1 + \dot{\Omega}_2}{\dot{\Omega}_1 + \dot{\Omega}_2} \right) L \tag{24b}$$

$$\dot{W}_{F2} = \frac{\bar{m}\sigma_0 R}{\sqrt{3}} \left(\dot{\Omega}_2^2 \frac{\lambda - 1}{\dot{\Omega}_1 + \dot{\Omega}_2} \right) L \tag{24c}$$

$$\dot{W}_D = \frac{\sigma_0}{\sqrt{3}} h_e L \dot{\Omega}_2 \tag{24d}$$

in which $$\Theta = \left[\frac{\lambda + 1}{L} \ln \lambda \right]^2 + \left[\frac{\lambda (\lambda - 1)}{(\lambda + 1) h_e} \Delta \right]^2$$

From the above expressions, the two torques are readily derived:

$$C_1 = \frac{\sigma_0}{\sqrt{3}} \frac{\lambda (\lambda - 1)^2}{(\lambda + 1) h_e} RL \frac{2\dot{\Omega}_2^2}{\left(\dot{\Omega}_1 + \dot{\Omega}_2 \right)^2} \Delta \Theta^{-1/2} + \\ + \frac{\bar{m}\sigma_0 RL}{\sqrt{3}} \left(1 - 2\dot{\Omega}_2^2 \frac{\lambda - 1}{\left(\dot{\Omega}_1 + \dot{\Omega}_2 \right)^2} \right) \tag{25a}$$

$$C_2 = \frac{\sigma_0}{\sqrt{3}} \frac{(\lambda + 1)}{\lambda} h_e RL \Theta^{1/2} \\ \left\{ 1 - \Theta^{-1} \left[\left(\frac{\lambda (\lambda - 1)}{(\lambda + 1) h_e} \right)^2 \frac{2\dot{\Omega}_1 \dot{\Omega}_2}{\left(\dot{\Omega}_1 + \dot{\Omega}_2 \right)^2} \Delta \right] \right\} + \ldots \\ \frac{\bar{m}\sigma_0 RL}{\sqrt{3}} \left[1 + (\lambda - 1) \frac{\dot{\Omega}_1^2 - \dot{\Omega}_2^2 - 2\dot{\Omega}_1 \dot{\Omega}_2}{\left(\dot{\Omega}_1 + \dot{\Omega}_2 \right)^2} \right] + \frac{\sigma_0 h_e L}{\sqrt{3}} \tag{25b}$$

It is also easy to derive the equivalent quantities pertaining to the case of symmetric rolling ($\dot{\Omega}_1 = \dot{\Omega}_2 = \dot{\Omega}$). In that case, there is a neutral point given by Eq. (17) for the two cylinders, and the friction power is given by

Eq. (18). Hence, setting Δ= a = 0 in Eqs (9), (18), and (20) above leads to the following expressions:

$$\dot{W}_p = \frac{\sigma_0}{\sqrt{3}} \frac{(\lambda+1)^2}{\lambda} \ln \lambda \dot{u}_e h_e \tag{26a}$$

$$\dot{W}_F = \frac{2\bar{m}\sigma_0}{\sqrt{3}} \frac{\left(\lambda^2+1\right)\dot{u}_e^2 - 2\dot{\Omega}R\left(\lambda+1\right)\dot{u}_e + 2\dot{\Omega}^2R^2}{2\left(\lambda-1\right)\dot{u}_e} L \tag{26b}$$

$$\dot{W}_D = \frac{\sigma_0}{\sqrt{3}} \frac{\dot{u}_e h_e L}{R} \tag{26c}$$

Minimization of the total power dissipated leads to:

$$\dot{u}_e^2 = \frac{2\bar{m}L\dot{\Omega}^2R^2}{\frac{(\lambda+1)^2(\lambda-1)\ln\lambda}{\lambda} h_e + \bar{m}L\left(\lambda^2+1\right) + \left(\lambda-1\right)\frac{h_e L}{R}} = \alpha^2\dot{\Omega}^2R^2 \tag{27}$$

and the rolling torque which, in this case, is common to the two cylinders, can be written in the form:

$$C = \frac{\sigma_0}{\sqrt{3}} \frac{(\lambda+1)^2}{\lambda} \ln\lambda \frac{\alpha R h_e}{2} + \frac{\left(\lambda^2+1\right)\alpha^2R/2 - (\lambda+1)\alpha R + R}{2(\lambda-1)\alpha} L + \frac{\sigma_0}{\sqrt{3}} \frac{h_e L}{R} \frac{\alpha R}{2} \tag{28}$$

The above predictions are illustrated in Figures 6a and b for r = 0.1 and 0.2, respectively. Note that $C_1 > 0$ and $C_2 < 0$, since the upper and lower cylinders are associated with driving work and resistant work, respectively, as stated above. In the case of symmetric rolling, the two cylinders are equivalent and exert globally a positive torque C on the sheet. For the two reduction ratios, C_1 and, to a lesser extent, $|C_2|$ are much larger than C. In fact, the above equations (25a) and (25b) are not applicable for $V_r > 0.8$, since the assumption $\dot{u}_e = \dot{\Omega}_2 R_2$ no longer holds. In that case, numerical calculations based on a more detailed velocity field have brought into evidence a smooth transition of C_1 and C_2 to their common value C [to be published].

Only a few number of former publications can be used for comparison with the above results, since they deal most generally with weakly asymmetric rolling ($0.8 < V_r < 0.9$) of thin sheet (h_e is small). Nevertheless, a slab model proposed by Tzou an co-workers [10, 11] leads to predictions in close agreement with the present ones, although it is strictly speaking only applicable to thin sheet since the plastic power is not readily taken into account. The authors give closed form equations for the two torques C_1 and C_2, although the diagrams display only the total torque $C=C_1+C_2$. This quantity does not appear to be quite significant, in particular because C_1 and C_2 have opposite signs and similar absolute values over almost the whole variation range of V_r, such that C is close to zero (Fig. 6).

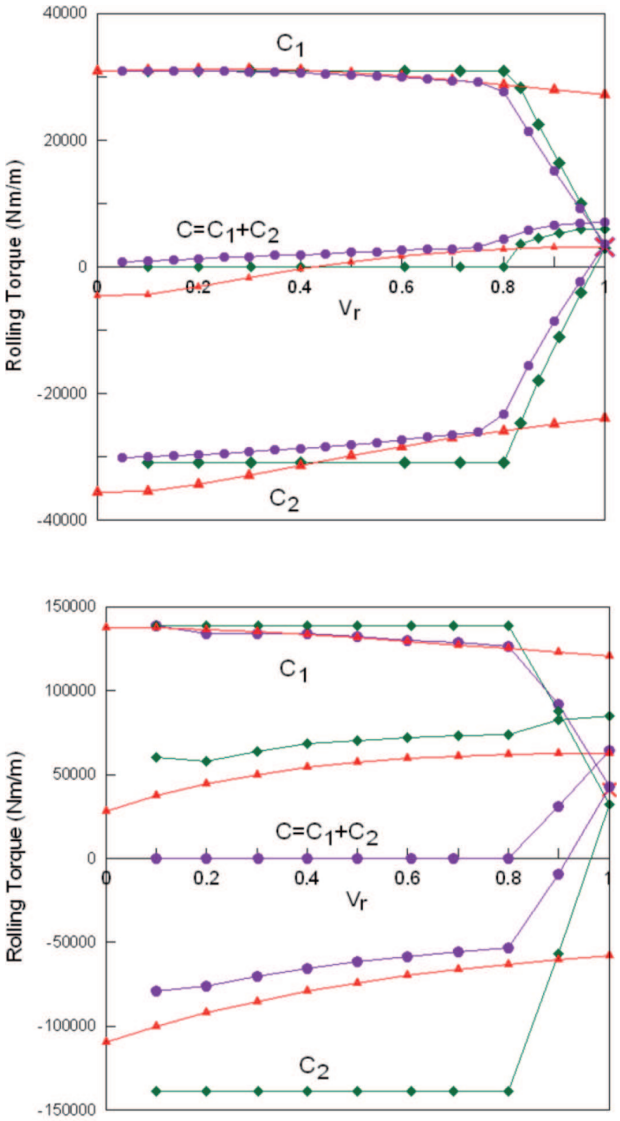

Fig. 6. Influence of the roll rotation velocity ratio on the two rolling torques C_1 and C_2 for (a) the ASR of a thin sheet (h_e = 0.5 mm), and (b) the ASR of a thick sheet (h_e= 10 mm). Three series of results are compared: predictions of the present model (circles), predictions assuming $\dot{u}_e = \dot{\Omega}_2 R_2$ (triangles), and Tzou's predictions (lozenges). The total torque $C = C_1 + C_2$ is also shown

The individual torques predicted by Tzou et al. [10, 11] were also plotted in Fig. 6 according to their equations, which shows that the upper one C_1 is almost equivalent to the present results for two initial sheet thicknesses h_e = 0.5 mm and 10 mm. C_2 is also similar for the thin sheet but the present approach predicts much smaller absolute values for h_e = 10 mm. It was checked that the power dissipated by the velocity discontinuity, which is neglected by Tzou *et al.* [10, 11], explains a small part of the discrepancy. It is thought that the major part of the latter has to be ascribed to plastic power, which is not included in the slab approach: in such conditions,

the lower (and slower) roll must exert larger torque to oppose the sheet velocity.

In another paper published by Farhat-Nia *et al.* [14], elastoplastic finite element simulations of asymmetric plate rolling have been carried out using an ALE approach. In the case of weakly asymmetric rolling ($0.93<V_r<1$), the authors computed an average rolling torque, which was assimilated here to the arithmetic average $C_{av} = (|C_1| + |C_2|)/2$. An alternative definition could be used as well by taking the average rotation velocity of the rolls associated with power conservation, which leads to $C'_{av} = (|C_1| + |C_2|\,V_r)/(1 + V_r)$. However, C_{av} and C'_{av} are quite similar for values of V_r close to unity. Since Coulomb friction with $\mu = 0.1$ was assumed, an equivalent Tresca coefficient was estimated from Tzou [11], *viz.* $\bar{m} = 0.25$. Finally, an average material flow stress was determined from the strain hardening equation used by the authors. Results in fairly good agreement with the present predictions are exhibited in Fig. 7 for three values of the reduction ratio r. It is worth to emphasize again, however, that the average torque is not physically meaningful nor practically useful, by contrast with the separate torques C_1 and C_2.

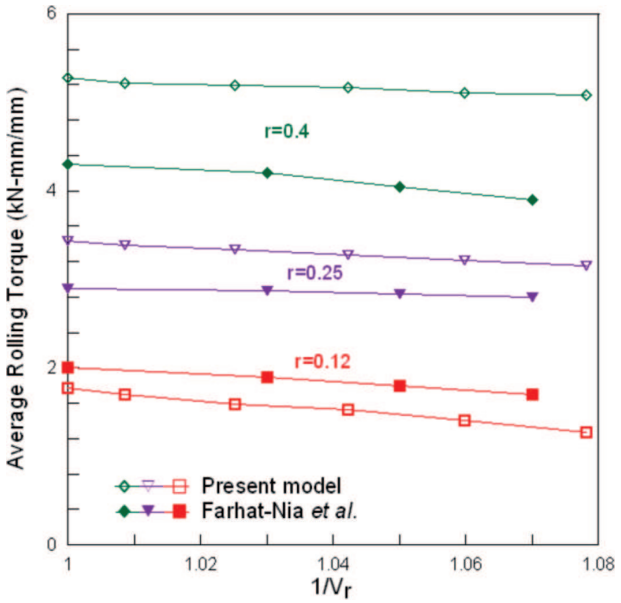

Fig. 7. Influence of the roll rotation velocity ratio on the average rolling torques. Three series of results for different r values are compared with results of Farhat-Nia *et al.* [14]

Comparison with other models involving strain rate sensitive materials are left for a next paper, where the extension of the present model to viscoplasticity will be proposed.

4. Conclusions

In this work, an original model of asymmetric rolling was proposed, based on a simple uniform strain field involving as single parameter the entry velocity of the sheet $\dot{u}_e$. The model can account for dissimilar cylinder radii and rotation velocities, as well as different friction coefficients between the sheet and the two rolls. However, the main results are related to the most common case of equal radius cylinders with maximum friction coefficient $\bar{m}$=1:

(i) When the ratio V_r of the rotation rates decreases, i.e. for larger asymmetry, the shear strain imposed to the sheet increases, but remains lower than the normal strain.

(ii) This requires much larger total power, although the two torques exerted by the cylinders remain almost constant when V_r is less than about 0.8.

(iii) In the same range of variation of V_r, the entry velocity of the sheet reasonably coincides with the outer linear velocity of the slower cylinder. This leads to closed form formulae for the two torques.

(iv) The above predictions are in good agreement with former work using the slab method. However, since the plastic power is readily taken into account, the present model can be applied to thick sheet and not only to thin sheet rolling, where friction effects are by far predominant. Also, the two torques can be predicted separately.

(v) Finally, due to its simplicity, this model precludes the determination of strain or stress gradients, as well as the rolling force. Such problems can be addressed by a more refined approach using velocity fields based on the material flow lines which will be shortly published.

Acknowledgements

The authors whish to thank the French ANR (”Programme Blanc”) which supported financially this research program.

APPENDIX A

Derivation of the roll gap length

An asymmetric rolling pass is geometrically defined by the two cylinder radii R_1 and R_2, and the initial (entry) thickness he and the final thickness h_f of the sheet (Figure A1).

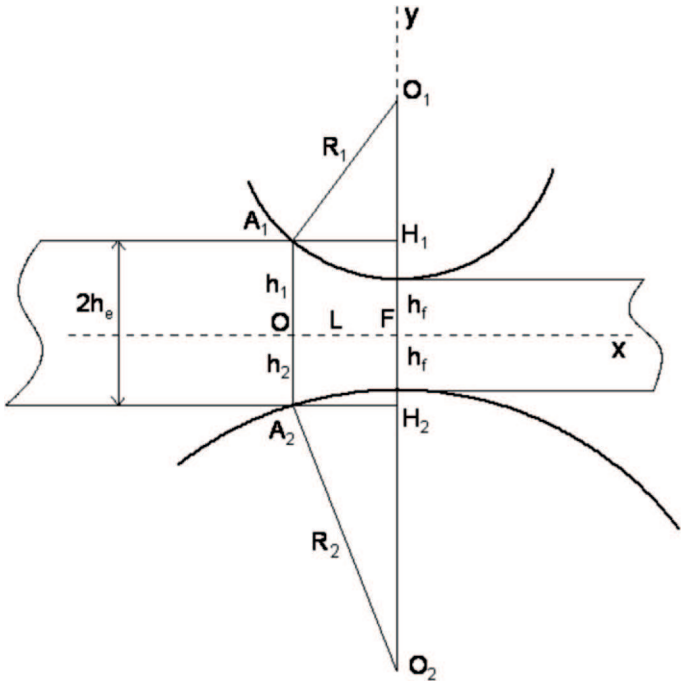

Fig. A1. Schematic representation of ASR including the definition of the various geometrical parameters

The two square triangles $O_1A_1H_1$ and $O_2A_2H_2$ verify:

$$L^2 = R_1^2 - (R_1 - h_1 + h_f)^2 \tag{A1a}$$

$$L^2 = R_2^2 - (R_2 - h_2 + h_f)^2 \tag{A1b}$$

where from:

$$h_2 - h_1 = \frac{-2\left(h_e - h_f\right)(R_2 - R_1)}{R_1 + R_2 - 2\left(h_e - h_f\right)} \tag{A2}$$

Combining this equation with:

$$h_1 + h_2 = 2h_e \tag{A4}$$

allows to derive h_1 and h_2:

$$h_1 = \frac{2h_eR_2 - h_f(R_2 - R_1) - 2h_e\left(h_e - h_f\right)}{R_1 + R_2 - 2\left(h_e - h_f\right)} \tag{A5a}$$

$$h_2 = \frac{2h_eR_1 + h_f(R_2 - R_1) - 2h_e\left(h_e - h_f\right)}{R_1 + R_2 - 2\left(h_e - h_f\right)} \tag{A5b}$$

Finally, substituting h_1 into (A1a) or h_2 into (A1b) gives:

$$L^2 = \frac{4\delta\left[-\delta^3 + 2(R_1 + R_2)\delta^2 - \left(R_1^2 + R_2^2 + 3R_1R_2\right)\delta + R_1R_2(R_1 + R_2)\right]}{(R_1 + R_2 - 2\delta)^2} \tag{A6}$$

in which $\delta = h_e - h_f$.

In the case where $R_1 = R_2 = R$, Eq. (A6) takes the simple form:

$$L^2 = \delta(2R - \delta) \tag{A7}$$

APPENDIX B

Estimation of the equivalent strain in asymmetric rolling

Consider a homogeneous plane strain incompressible deformation path that transforms the square OABC into the parallelogram OA'B'C' (Figure B1).

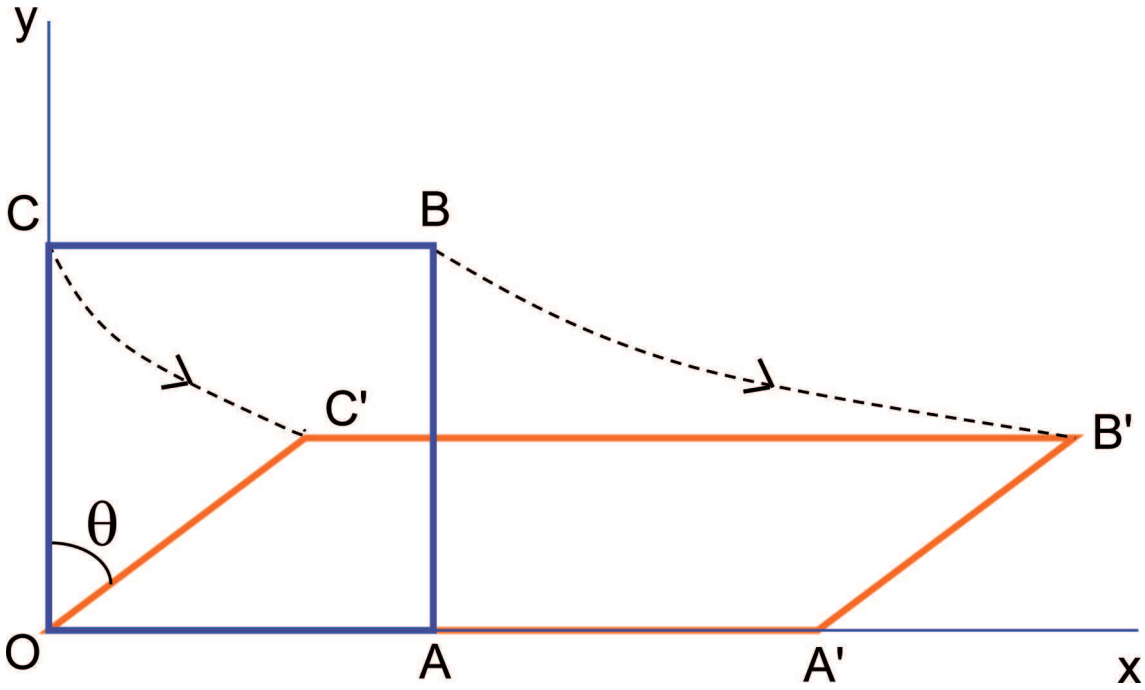

Fig. B1. Schematic illustration showing the transformation of a material element during a pass of ASR

The associated velocity field takes the general form:

$$\begin{cases} u_x = \dot{\varepsilon} x + \dot{\gamma} y \\ u_y = -\dot{\varepsilon} y \end{cases} \tag{B1}$$

In the special case of steady state flow, $\dot{\varepsilon}$ and $\dot{\gamma}$ are independent of time. The flow lines (trajectories) are derived by solving the following set of differential equations:

$$\begin{cases} \dfrac{dx}{dt} = \dot{\varepsilon} x + \dot{\gamma} y \\ \dfrac{dy}{dt} = -\dot{\varepsilon} y \end{cases} \tag{B2}$$

The general solution is:

$$\begin{cases} y = y_{0\exp(-\varepsilon)} \\ x = \left(x_0 + \dfrac{a}{2} y_0\right) \exp(\varepsilon) - \dfrac{a}{2} y_0 \exp(-\varepsilon) \end{cases} \tag{B3}$$

in which (x_0, y_0) denotes the initial position of a material point, and $\varepsilon = \dot{\varepsilon} t$. Elimination of the strain ε leads to the equation of the hyperbolic flow line:

$$\frac{a}{2}\left(y^2 - y_0^2\right) + xy - x_0 y_0 = 0 \tag{B4}$$

one asymptote of which coincides with the x-axis, the second one being inclined towards the negative x-axis with slope – 2/a.

The *apparent shear strain* of a material element is given by the angle between OC′ and the y-axis. The coordinates of C′ are obtained by setting $x_0 = 0$ in Eqs (B3).

Hence:

$$\gamma_{app} = \tan\theta = \frac{a}{2}\left[\exp(2\varepsilon) - 1\right] \tag{B5}$$

or, since ε=lnλ:

$$\gamma_{app} = \frac{a}{2}\left(\lambda^2 - 1\right) = a\frac{r(2-r)}{2(1-r)^2} \tag{B6}$$

where r=1–1/λ. This equation was proposed by Saito *et al.* [20].

REFERENCES

[1] A. Wauthier, H. Réglé, J. Formigoni, G. Herman, Mater. Char. **60**, 90-95 (2009).
[2] Y.H. Ji, J.J. Park, W.J. Kim, Mater. Sci. Eng. **A 454–455**, 570–574 (2007).
[3] G. Sachs, L.J. Klinger, ASME J.Appl. Mech. **69**, 88–98 (1947).
[4] R.L. Holbrook, C.F. Zorowski, ASME J. Eng. Ind. **B 88**, 401–409 (1966).
[5] S.A. Buxton, S.C. Browning, J. Mech. Eng. Sci. **14**, 245-254 (1972).
[6] A.P. Chekmarev, A.A. Nefedov, Obrabotka Metallov Davleniem **4(2)**, 1956 (British Library Translation R.T.S. 8939).
[7] M.I. Ghobrial, Int. J. Mech. Sci. **34**, 757-764 (1989).
[8] Y.M. Hwang, T.H. Chen, H.H. Hsu, Int. J. Mech. Sci. **38**, 443-460 (1995).
[9] Y.M. Hwang, G.Y. Tzou, Int. J. Mech. Sci. **39**, 289-303 (1997).
[10] Y.M. Hwang, G.Y. Tzou, J. Mater. Proc. Technol. **52**, 399-424 (1994).
[11] G.Y. Tzou, J. Mater. Process. Technol. **86**, 271-277 (1999).
[12] M. Salimi, F. Sassani, Int. J. Mech. Sci. **44**, 1999-2023 (2002).
[13] M. Salimi, M. Kadkhodaei, J. Mater. Proc. Technol. **150**, 215-222 (2004).
[14] F. Farhat-Nia, M. Salimi, M.R. Movahhedy, J. Mater. Proc. Technol. **177**, 525-529 (2006).
[15] M. Kadkhodaei, M. Salimi, M. Poursina, Int. J. Mech. Sci. **49**, 622-634 (2007).
[16] A.B. Richelsen, Int. J. Mech. Sci. **39**, 1199-1211 (1997).
[17] L.S. Lu, O.K. Harrer, W. Schwenzfeier, F.D. Fischer, Int. J. Mech. Sci. **42**, 49-61 (2000).
[18] S.A.A. Akbari Mousavi, S.M. Ebrahimi, R. Madoliat, J. Mater. Proc. Technol. **187-188**, 725-729 (2007).
[19] P. Baque, E. Felder, J. Hyafil, Y. D'Escatha, Mise en forme des metaux. Calculs par la plasticite, t.2, Dunod, Paris (1973).
[20] Y. Saito, T. Sakai, F. Maeda, K. Kato, J Iron Steel Inst. Jap. **72**, 799-806 (1986).
[21] Q. Cui, K. Ohori, Mater. Sci. Technol. **16**, 1095-1101 (2000).

Received: 20 November 2011.